Probabilistic quantification of regional cortical microstructural complexity

H. A. Haroon[1,2], R. J. Binney[2,3], and G. J. Parker[1,2]

[1]Imaging Science and Biomedical Engineering, School of Cancer and Imaging Sciences, The University of Manchester, Manchester, England, United Kingdom, [2]The University of Manchester Biomedical Imaging Institute, The University of Manchester, Manchester, England, United Kingdom, [3]Neuroscience and Aphasia Research Unit, School of Psychological Sciences, The University of Manchester, Manchester, England, United Kingdom

Introduction The application of model-based residual (MBR) bootstrapping to the constrained spherical deconvolution[1] (CSD) analysis of HARDI data allows us to obtain probabilities of observing n fiber orientations on a voxel-by-voxel basis[2,3]. We hypothesized that the distribution of these probabilities for each n within regions defined by segmentation and parcellation of cortical and subcortical structures would reflect the varying underlying neural microstructural complexity associated with each. Here we present example voxelwise probabilistic maps of observing n fiber orientations over 100 MBR iterations and show corresponding maps of the median of the distribution of probabilities for each n within a sample from 86 cortical and subcortical regions. We also show the consistency of the inter-region medians between hemispheres and the correlation between subjects, indicating that DWI-derived cortical complexity measurements are sensitive to the different microstructural arrangements of different cortical regions and that they may provide a mechanism for non-invasive cytoarchitectonic assessment.

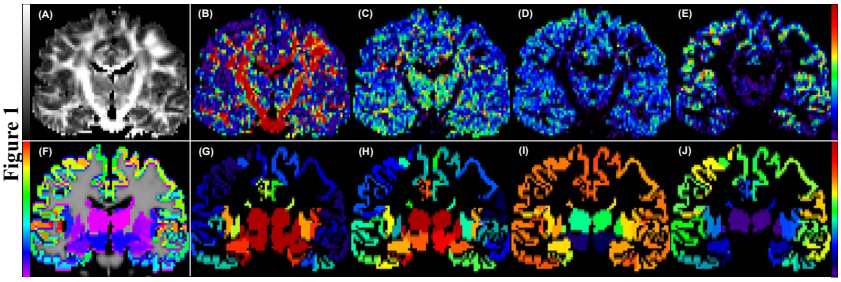

Figure 1

Methods *Imaging:* High-resolution anatomical T_1-weighted data followed by HARDI were acquired in five healthy male subjects [subject 1 was 37 years of age; subjects 2–4 were 20; subject 5 was 23] on a 3T Philips Achieva scanner (Philips Healthcare, Best, Netherlands) using an 8-element head coil. T_1: 3D Turbo Field Echo Inversion Recovery with TE = 3.9 ms, TR = ~2000 ms, TI = 1150 ms, 256 × 205 matrix reconstructed to 256 × 256, reconstructed resolution 0.938 × 0.938 mm^2, slice thickness 0.9 mm, 160 contiguous slices, SENSE factor = 2.5. HARDI: PGSE EPI with TE = 59 ms, cardiac gating, G_{max} = 62 mT/m, partial Fourier factor 0.679, 112 × 112 matrix reconstructed to 128 × 128, reconstructed resolution 1.875 × 1.875 mm^2, slice thickness 2.1 mm, 60 contiguous slices, 61 diffusion sensitization directions at b = 1200 s/mm^2 (Δ = 29.8 ms, δ = 13.1 ms), 1 at b = 0, SENSE factor = 2.5, correction for susceptibility and eddy current-induced distortion[4]. *Cortical and Subcortical Parcellation:* We ran FreeSurfer's (surfer.nmr.mgh.harvard.edu) fully automated brain extraction, tissue segmentation[5] and parcellation[6] software on the high-resolution T_1-weighted volume for each subject. We used 34 cortical regions in each hemisphere, which were anatomically defined and covered all of the cerebral cortex, and 9 subcortical gray matter regions in each hemisphere. The b = 0 volume for each subject was registered to the extracted T_1-weighted brain volume for that subject by implementing affine registration in FSL's (www.fmrib.ox.ac.uk/fsl) FLIRT[7]. The transformation matrix obtained was inverted and then applied to the parcellation volume from FreeSurfer, so that the parcellation volume would be in the same frame of reference as the subject's HARDI data. *Constrained Spherical Deconvolution:* We implemented CSD[1] on the acquired HARDI data. The response function was obtained from the simulation of a single diffusion tensor with fractional anisotropy of 0.8 and b = 1200s/mm^2. The fiber orientation distribution (FOD) function was generated with 45 spherical harmonics (l_{max}=8) and was then reconstructed at 8000 equidistant points on the sphere, within each voxel. *MBR Bootstrapping:* In order to obtain residuals in a given voxel we spherically convolved the spherical harmonics of the FOD generated by CSD with the rotational harmonics of the response function. This gave us recovered HARDI signal, devoid of noise. Residuals were calculated by taking the difference between the recovered HARDI signal and the original HARDI signal. A new image set was created by randomly shuffling the residuals, for any given voxel, amongst all the diffusion-encoding directions and then adding them to the recovered HARDI signals. The image set created by each bootstrap sampling was then processed with CSD to generate new instances of the FODs. To further minimize the effects of noise we set a threshold to only accept those peaks on the FOD, as relating to the principle underlying intravoxel fiber orientations (one or more), whose magnitude was greater than 70% of the maximum peak magnitude on the FOD, in a given voxel. *Probability of Number of Fiber Populations:* The probability of observing n fiber orientations ($n \in [1, 2, 3, >3]$) was determined from the frequency of finding n fiber orientations over 100 MBR bootstrap iterations. *Probability Distribution in Parcellated Regions:* The median was calculated as the descriptor of the distribution of probabilities of n fiber orientations amongst all the voxels within each of the cortical and subcortical parcellated regions. In order to demonstrate inter-subject consistency we plotted the parcellation medians for one subject against each of the other subjects, and also plotted the group medians of the parcellation medians across all five subjects for the left hemisphere against the right to assess symmetry of cortical complexity. To obtain a statistical measure of inter-subject similarity we computed correlation coefficient matrices for the parcellation medians between all five subjects for each n and for cortical and subcortical regions separately. **Results** Various maps for a mid-volume coronal slice in one subject are shown in Figure 1. Fig. 1(A) shows an anisotropy map, followed by voxelwise maps of $P(n = 1)$, $P(n = 2)$, $P(n = 3)$ and $P(n > 3)$ (Fig. 1(B–E), respectively) over 100 MBR bootstrap iterations rendered with the same colormap scaled 0–100%. Color-rendered parcellation regions are overlaid on the corresponding contrast-reduced grayscale T_1-weighted image in Fig. 1(F), which is followed by maps of the parcellation medians in this subject for $P(n = 1)$, $P(n = 2)$, $P(n = 3)$ and $P(n > 3)$ (Fig. 1(G–J), respectively) rendered with the same colormap but individually windowed to aid visualization for qualitative comparison. The plots in Fig. 2 have used different marker types and colors to separate cortical and subcortical parcellation regions and median probabilities for each n. The strong correspondence between group medians of parcellation medians in the left and right hemispheres is clearly evident in Fig. 2(A). The parcellation medians in the first subject also correspond well with the parcellation medians in the other four subjects (Fig. 2(B-E)). All of the off-diagonal entries in the matrices of correlation coefficients in Fig. 3 are statistically significant (p<0.01), with correlation coefficients being generally higher for subcortical parcellation regions (Fig. 2(A,C,E,G)) than cortical regions (Fig. 2(B,D,F,H)). **Conclusion** We have successfully shown consistency in the probability of finding different fiber configurations within parcellated cortical and subcortical regions both between hemispheres and amongst a small group of healthy subjects. This suggests that applying model-based residual bootstrapping to the CSD analysis of clinically-acquirable HARDI data can elucidate information about the underlying microstructural complexity. This information represents a non-invasive measure that is sensitive to cortical cytoarchitecture and that may be useful in cortical parcellation and in the identification of cortical lesions.

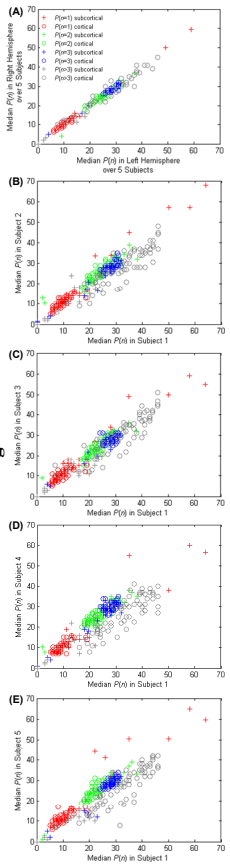

Figure 2

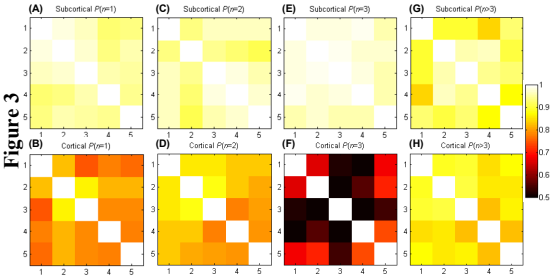

Figure 3

References 1) Tournier, J-D, *et al*, *NeuroImage*, **35**: 1459, 2007. 2) Haroon, HA, *et al*, *ISMRM*, 363, 2009. 3) Haroon, HA, *et al*, *IEEE Trans Med Imaging*, **28**:535, 2009. 4) Embleton, KV, *et al*, *Hum Brain Mapp*, in press, 2009. 5) Yeo, BTT, *et al*, *Med Image Anal*, **12**:603, 2008. 6) Fischl, B, *et al*, *Cereb Cortex*, **18**:1973, 2008. 7) Jenkinson, M, *et al*, *NeuroImage*, **17**:825, 2002.

Acknowledgements This work was supported by the UK's BBSRC (BB/E002226/1), EPSRC (GR/T02669/01) and MRC (G0501632).